Measurement of axial vector form factor using antineutrino-hydrogen scattering

Tejin Cai

University of Rochester
York University
for the MINERvA Collaboration

October 24, 2022

NuINT 2022

Outline

Introduction

The MINERvA Experiment

Study neutrino-nucleus scattering at the few-GeV region

- Precision measurements on signal and background processes in oscillation experiments
- Study nuclear effects to improve understanding of neutrino-nucleus cross section and modelling
- Demonstrate experimental techniques for current and future oscillation experiments
- ~ 40 measurements on hydrocarbon, heavy nuclei, and electrons
- Precise flux constraints[1,2]

High Resolution Scintillator(CH) Detector

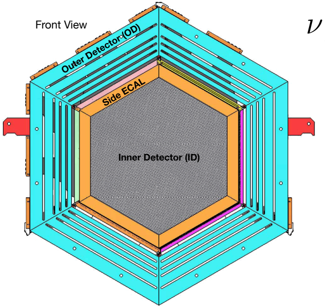

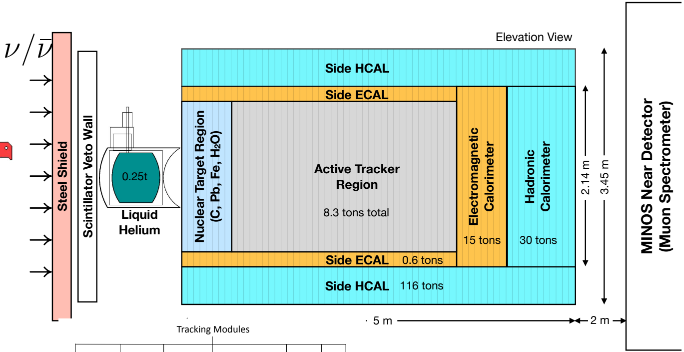

Nucl. Inst. and Meth. A743 (2014) 130.

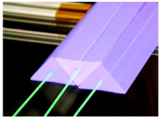

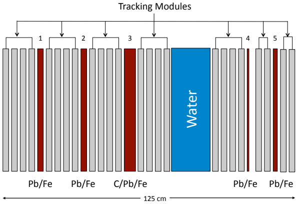

CH in tracker
Pb, Fe, C and water in target region
3.1 mm tracking resolution

Quasi-Elastic Scattering

- The very first results from MINERvA on hydrocarbon
- A main signal for oscillation experiments
- Simple final states

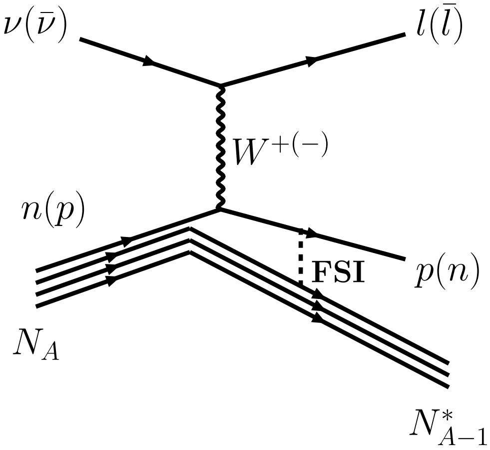

Quasi-Elastic Like Scattering

- The very first results from MINERvA on hydrocarbon
- A main signal for oscillation experiments
- Simple final states
- Nuclear effects complicate the matter

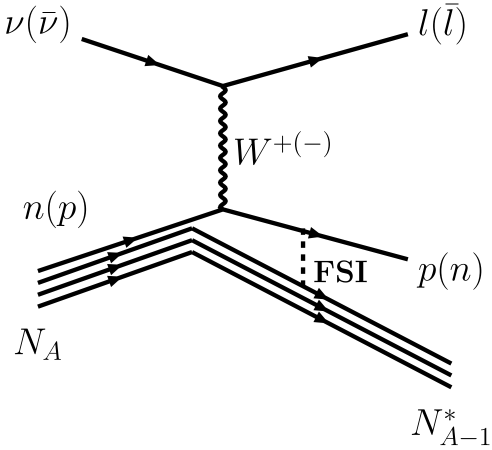

~~Quasi-~~Elastic Scattering

- The very first results from MINERvA on hydrocarbon
- A main signal for oscillation experiments
- Simple final states
- Nuclear effects complicate the matter
- Can we measure hydrogen?

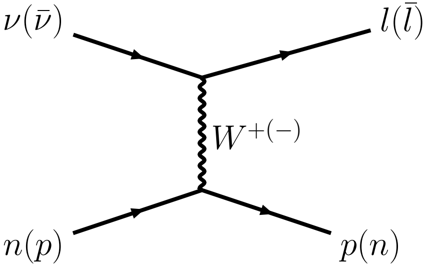

Free Nucleon Cross-Section: Llewllyn Smith Equations

$$\frac{\mathrm{d}\sigma}{\mathrm{d}Q^2}\begin{pmatrix}\nu n \to l^- p \\ \bar{\nu} p \to l^+ n\end{pmatrix} = \frac{M^2 G_F^2 \cos^2\theta_c}{8\pi E_\nu^2}\left[A(Q^2) \mp B(Q^2)\frac{(s-u)}{M^2} + C(Q^2)\frac{(s-u)^2}{M^4}\right], \tag{1}$$

$$\begin{aligned}
A(Q^2) &= \frac{m^2+Q^2}{4M^2}\Bigg[\left(4+\frac{Q^2}{M^2}\right)|F_A|^2 - \left(4-\frac{Q^2}{M^2}\right)|F_V^1|^2 \\
&\quad + \frac{Q^2}{M^2}\left(1-\frac{Q^2}{4M^2}\right)|\xi F_V^2|^2 + \frac{4Q^2}{M^2}\mathrm{Re}F_V^{1*}\xi F_V^2 + \mathcal{O}\left(\frac{m^2}{M^2}\right)\Bigg], \\
B(Q^2) &= \frac{Q^2}{M^2}\mathrm{Re}F_A^*(F_V^1+\xi F_V^2), \\
C(Q^2) &= \frac{1}{4}\left(|F_A|^2 + |F_V^1|^2 + \frac{Q^2}{4M^2}|\xi F_V^2|^2\right)
\end{aligned} \tag{2}$$

Functions of vector form factors (F_V^1, ξF_V^2) from electron scattering and axial-vector form factor (F_A) → No (significant) direct measurement on free proton.

Measure free proton cross-section with MINERvA

Measure the signal process (Charged Current Elastic scattering)

$$\bar{\nu}_\mu + p \to \mu^+ + n,$$

with the most intense antineutrino beam and a detector with a lot of free protons:

- POT:1.12×10^{21}
- No. of hydrogen atoms: $\sim 2.61 \times 10^{29}$

There is an equal number of carbon with more than $5\times$ more cross-section rate.

- But they have nuclear effects that alters the kinematics of the outgoing particles.
- Use neutrons to constrain this background

Neutron Reconstruction in MINERvA

Neutron Signature

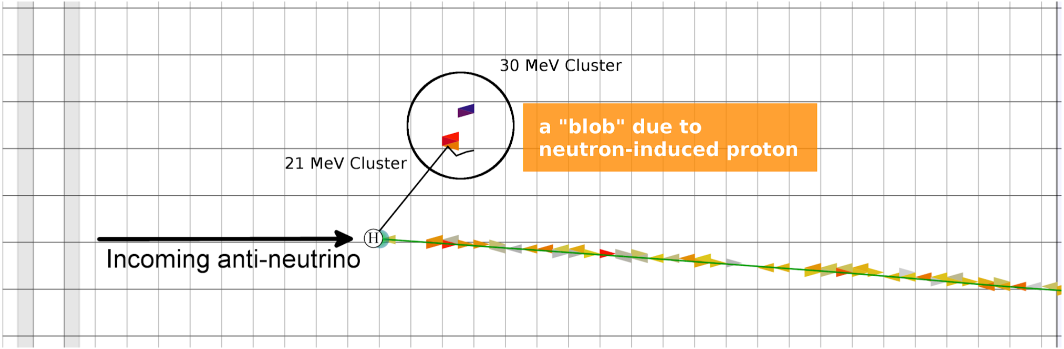

An incoming anti-neutrino scatters off a hydrogen producing neutron. The neutron undergoes secondary interactions to produce visible proton.

Using Nuclear Effects to Advantage

Assuming 2-body scattering, could calculate expected neutron direction:

$$p_{\mathrm{n}}^{\parallel} = \frac{M_{\mathrm{n}}^2 + {p_{\mu}^{\perp}}^2 - (p_{\mu}^{\parallel} - E_{\mu} + M_{\mathrm{p}})^2}{2(p_{\mu}^{\parallel} - E_{\mu} + M_{\mathrm{p}})^2},$$

$$\vec{p}_{\mathrm{n}}^{\perp} = -\vec{p}_{\mu}^{\perp}$$

Capture deviations in carbon using the following angular variables: $\hat{z}' = \hat{t}$, $\hat{x}' = \hat{p}_{\nu} \times \hat{p}_{\mu}$, $\hat{y}' = \hat{z}' \times \hat{x}'$,

$$\delta\theta_{\mathrm{P}} = \arctan\left(\hat{n}\cdot\hat{x}'/\hat{n}\cdot\hat{z}'\right),$$

$$\delta\theta_{\mathrm{R}} = \arctan\left(\hat{n}\cdot\hat{y}'/\hat{n}\cdot\hat{z}'\right)$$

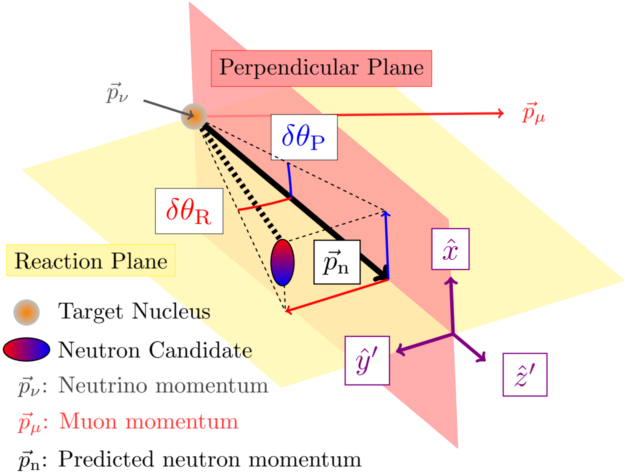

Simulation and Event Selection

Signal Definition and Base Model

Event topology:

- 1 μ^+ and no trackable hadrons

Muon acceptance due to detector geometry:

- $1.5\ \mathrm{GeV} < E_\mu < 20\ \mathrm{GeV}$
- $\theta_\mu < 20^\circ$ wrt to neutrino beam

Neutron selection:

- ≥ 1 3D neutron candidate
- Leading 3D energy deposits $10\mathrm{mm}$ away from the muon axis.

Cross section variable: Q^2, signal process:
$\bar{\nu} + H \rightarrow \mu^+ + n$

Base Model Composition:

- MnvGENIE-v2.5.1
  - Nieves 2p2h[3] and low-recoil tune[4]
  - RPA tune[5]
  - Non-resonant Pion Reduction[6]
  - Low-Q^2 resonant pion suppression[7]
  - Carbon elastic FSI reweight[8]
  - CCQE carbon NuWro SF reweight[9,10]
- A GEANT4 neutron reweight[11,12]

QELike Selection for $\bar{\nu}$

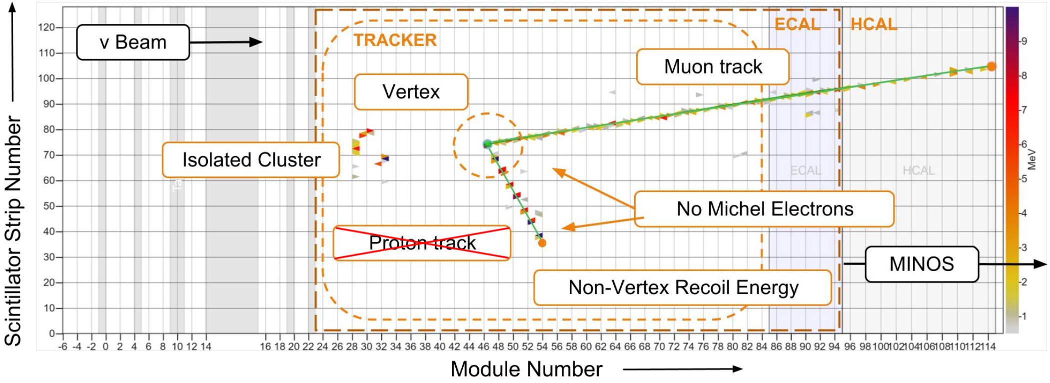

Like a typical ν QELike, but without any hadronic tracks.
Recoil energy follows a Q^2-dependent cut

Condition	E_{max}^{recoil} (GeV)
$Q^2_{QE} < 0.3\ (\mathrm{GeV}/c)^2$	$0.04 + 0.43Q^2_{QE}/(\mathrm{GeV}/c)^2$
$Q^2_{QE} < 1.4\ (\mathrm{GeV}/c)^2$	$0.08 + 0.3Q^2_{QE}/(\mathrm{GeV}/c)^2$
$Q^2_{QE} > 1.4\ (\mathrm{GeV}/c)^2$	0.50

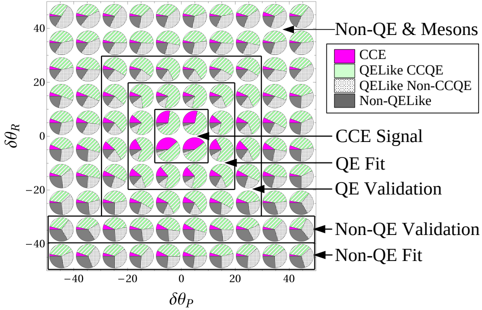

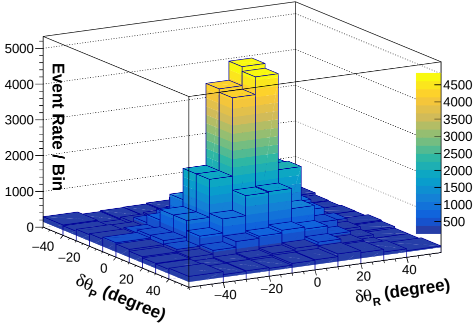

(left) Angular regions and MC event fraction, (right) total data event rate

- Hydrogen events ~ 30% of events in the central region
- Carbon QELike (CCQE) larger spreads
- Carbon QELike (non-CCQE) wider

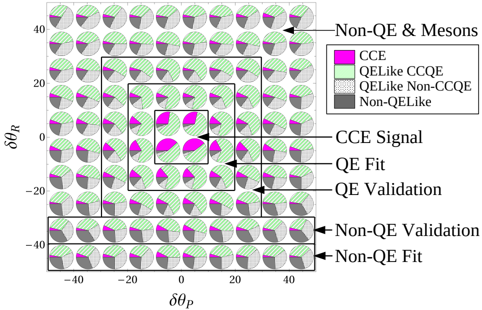

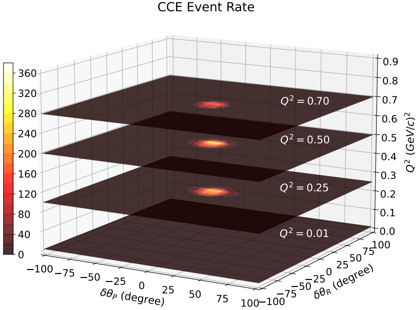

(left) Angular regions and MC event fraction, (right) MC events in slices of Q^2

- Hydrogen events $\sim 30\%$ of events in the central region
- Carbon QELike (CCQE) larger spreads
- Carbon QELike (non-CCQE) wider

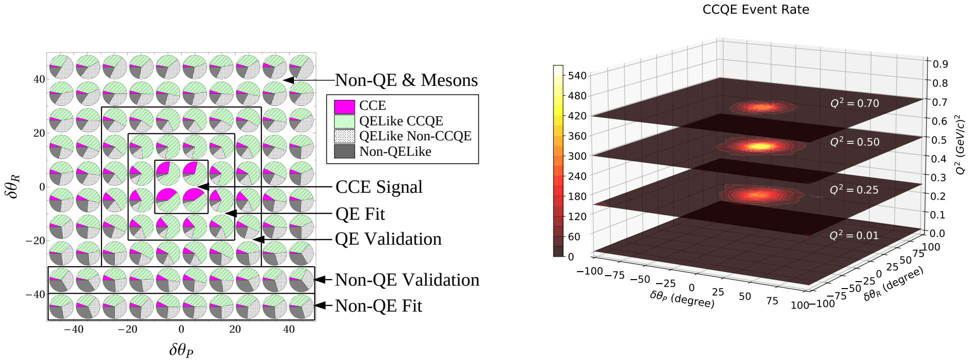

(left) Angular regions and MC event fraction, (right) MC events in slices of Q^2

- Hydrogen events $\sim 30\%$ of events in the central region
- Carbon QELike (CCQE) larger spreads
- Carbon QELike (non-CCQE) wider

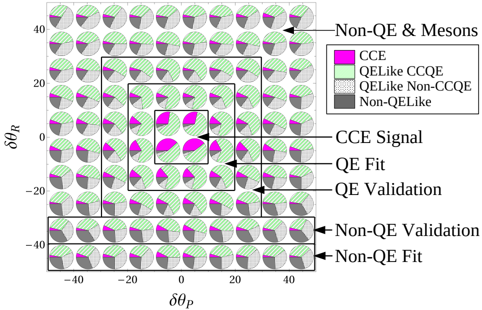

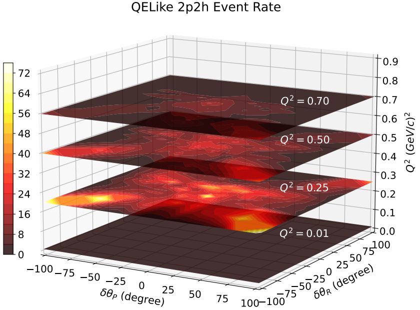

(left) Angular regions and MC event fraction, (right) MC events in slices of Q^2

- Hydrogen events $\sim 30\%$ of events in the central region
- Carbon QELike (CCQE) larger spreads
- Carbon QELike (non-CCQE) wider

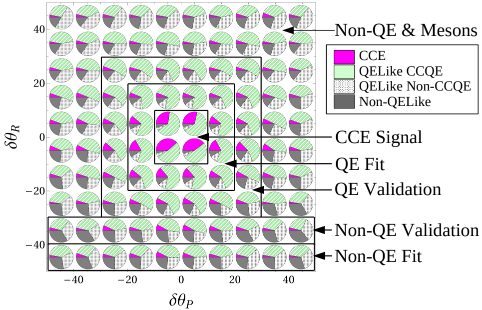

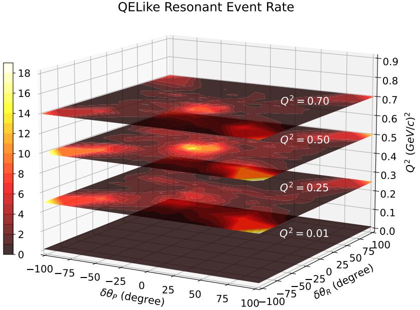

(left) Angular regions and MC event fraction, (right) MC events in slices of Q^2

- Hydrogen events $\sim 30\%$ of events in the central region
- Carbon QELike (CCQE) larger spreads
- Carbon QELike (non-CCQE) wider

Cross-section Extraction

Event Rate with Constrained Backgrounds

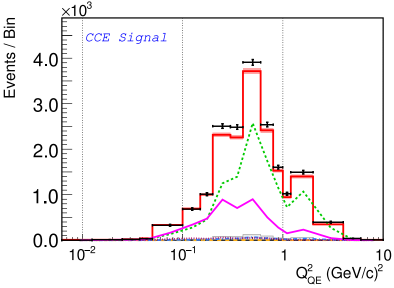

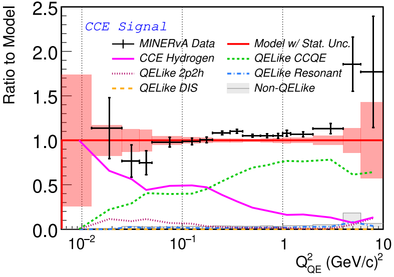

Figure: Event rate and ratio in CCE region

CCE is the signal , CCQE is the dominant background. Unfolding of the background subtracted signal done with D'agostini and 4 iterations.

Event Rate with Constrained Backgrounds

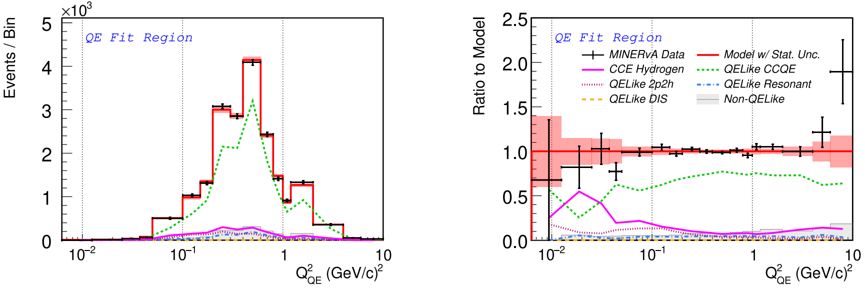

Figure: Event rate and ratio in CCQE-Fit region

CCE is the signal , CCQE is the dominant background. Unfolding of the background subtracted signal done with D'agostini and 4 iterations.

Efficiency

- Low Q^2: Low acceptance because neutron needs to produce protons that span at least 2 planes.
- high Q^2: Reconstruction inefficiency and larger opening angles and less detector material to contain neutrons.

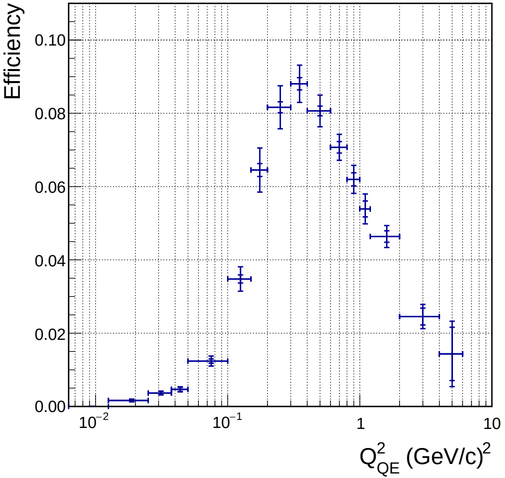

Cross-section and fitting F_{A}

Cross-section prediction

- Needs to account for muon acceptance
- Pre-calculate LS equation by factoring out vector form factors
- We use BBBA2005[13] parameterization
- F_A fit assumes z-expansion form[14].

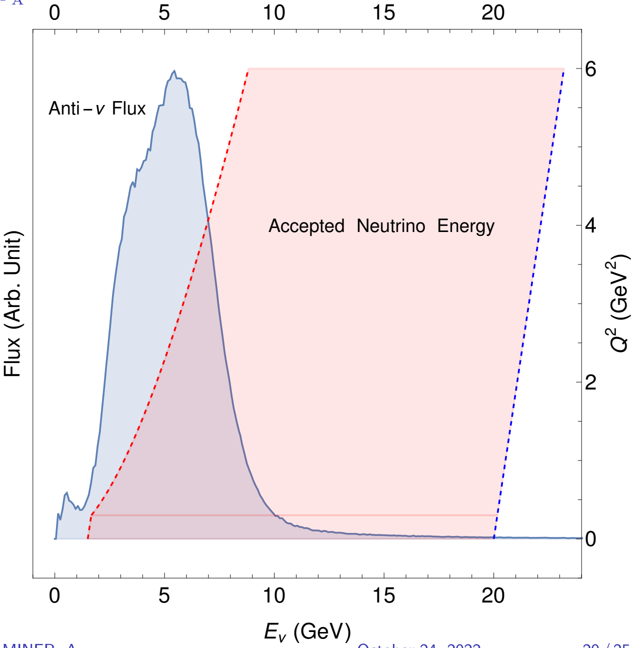

Deuterium Fit[14], BBBA2007[15]

Cross-section

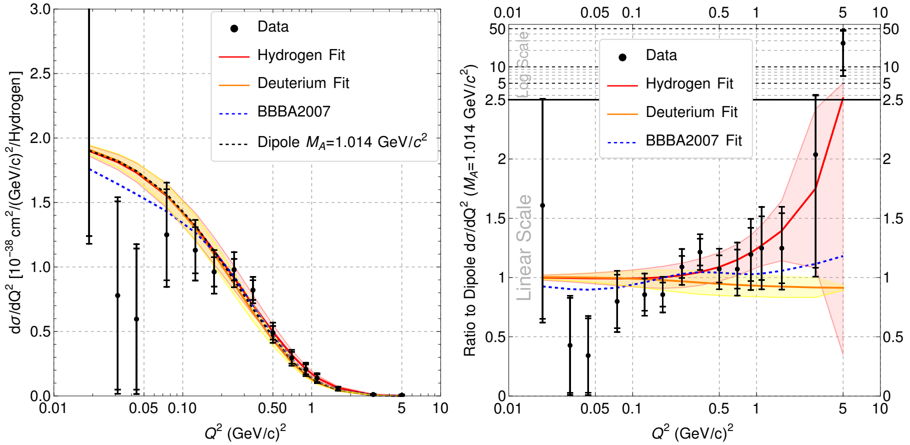

Figure: Extracted cross-section and ratio to a dipole form factor.

Total sysytematics

- Dominated by statistical uncertainty from background subtraction, despite enhanced signal
- Systematic uncertainties from residuals of background subtraction

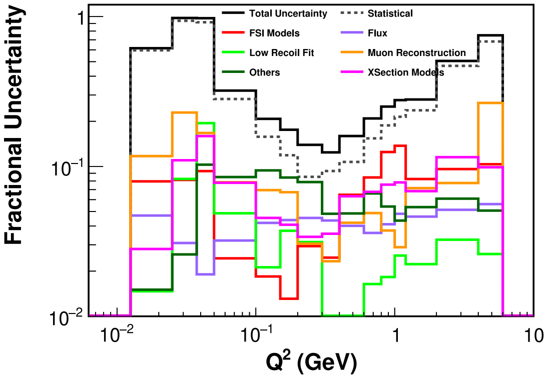

F_A fit and axial radius of the proton

Favors larger F_A at higher Q^2.
If fit with dipole, $M_A \sim 1.15(10)$

Calculate proton radius from F_A

$$F_A(Q^2) = F_A(0)\left(1 - \frac{\langle r_A^2\rangle}{3!}Q^2 + \frac{\langle r_A^4\rangle}{5!}Q^4 + \dots\right),$$

$$\frac{1}{F_A(0)}\frac{dF_A}{dQ^2}\bigg|_{Q^2=0} = -\frac{1}{6}\langle {r_A}^2\rangle$$

- $\sqrt{\langle r_A^2\rangle} = 0.73(17)\mathrm{fm}$

Deuterium Fit[14], BBBA2007[15], LQCD[16]

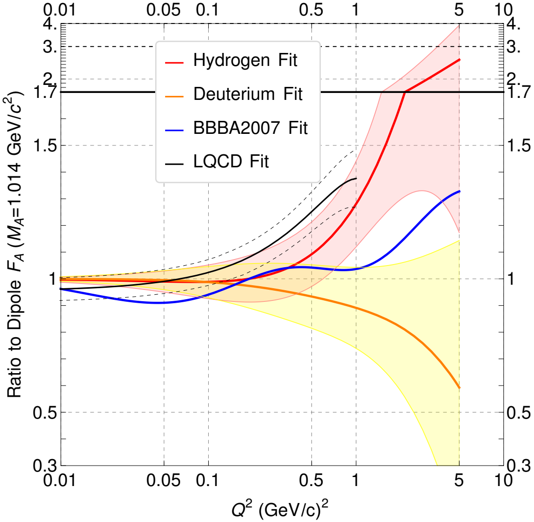

Conclusion

Performed the only statistically significant measurement of free proton using a weak probe. The result is presented publicly for the first time here.

- Developed algorithms to tag neutron candidates and used their directions to constrain interactions on carbon.
- Extracted the $\bar{\nu}_\mu H$ CCE cross-section, using the hydrocarbon target in MINERvA
- Fitted the cross-section to an z-expansion axial form factor with BBBA2005 vector form factors.
- Resulting fit favors larger values of F_{A} at $Q^2 > 1\,\mathrm{GeV}^2$ compared to a dipole form factor with $M_A = 1.014\,\mathrm{GeV}$. Proton radius from F_{A} consistent with electron scattering experiments.

Thank you!

Reference I

[1] E. Valencia et al. "Constraint of the MINERνA medium energy neutrino flux using neutrino-electron elastic scattering". In: *Phys. Rev. D* 100.9 (2019), p. 092001. DOI: 10.1103/PhysRevD.100.092001. arXiv: 1906.00111 [hep-ex].

[2] L. Zazueta et al. "Improved constraint on the MINERvA medium energy neutrino flux using $\bar{\nu} e^- \rightarrow \bar{\nu} e^-$ data". In: (Sept. 2022). arXiv: 2209.05540 [hep-ex].

[3] J. Nieves, I. Ruiz Simo, and M. J. Vicente Vacas. "Inclusive Charged–Current Neutrino–Nucleus Reactions". In: *Phys. Rev.* C83 (2011), p. 045501. DOI: 10.1103/PhysRevC.83.045501. arXiv: 1102.2777 [hep-ph].

Reference II

[4] P. A. Rodrigues, J. Demgen, E Miltenberger, et al. "Identification of Nuclear Effects in Neutrino-Carbon Interactions at Low Three-Momentum Transfer". In: *Phys. Rev. Lett.* 116 (7 Feb. 2016), p. 071802. DOI: 10.1103/PhysRevLett.116.071802. URL: https://link.aps.org/doi/10.1103/PhysRevLett.116.071802.

[5] J. Nieves, Jose Enrique Amaro, and M. Valverde. "Inclusive quasi-elastic neutrino reactions". In: *Phys. Rev.* C70 (2004). [Erratum: Phys. Rev.C72,019902(2005)], p. 055503. DOI: 10.1103/PhysRevC.70.055503,10.1103/PhysRevC.72.019902. arXiv: nucl-th/0408005 [nucl-th].

Reference III

[6] Philip Rodrigues, Callum Wilkinson, and Kevin McFarland. "Constraining the GENIE model of neutrino-induced single pion production using reanalyzed bubble chamber data". In: *Eur. Phys. J.* C76.8 (2016), p. 474. DOI: 10.1140/epjc/s10052-016-4314-3. arXiv: 1601.01888 [hep-ex].

[7] P. Stowell et al. "Tuning the genie pion production model with MINERvA data". In: *Physical Review D* 100.7 (Oct. 2019). ISSN: 2470-0029. DOI: 10.1103/physrevd.100.072005. URL: http://dx.doi.org/10.1103/PhysRevD.100.072005.

[8] L. A. Harewood and R. Gran. "Elastic hadron-nucleus scattering in neutrino-nucleus reactions and transverse kinematics measurements". In: (2019). arXiv: 1906.10576 [hep-ex].

Reference IV

[9] Artur M. Ankowski and Jan T. Sobczyk. "Construction of spectral functions for medium-mass nuclei". In: *Phys. Rev.* C77 (2008), p. 044311. DOI: 10.1103/PhysRevC.77.044311. arXiv: 0711.2031 [nucl-th].

[10] C. Juszczak, J. A. Nowak, and J. T. Sobczyk. "Spectrum of recoil nucleons in quasi-elastic neutrino nucleus interactions". In: *Eur. Phys. J. C* 39 (2005), pp. 195–200. DOI: 10.1140/epjc/s2004-02086-9.

[11] A. Del Guerra. "A compilation of n-p and n-C cross sections and their use in a Monte Carlo program to calculate the neutron detection efficiency in plastic scintillator in the energy range 1–300 MeV". In: *Nuclear Instruments and Methods* 135.2 (1976), pp. 337–352. ISSN: 0029-554X. DOI: https://doi.org/10.1016/0029-554X(76)90181-6. URL: https://www.sciencedirect.com/science/article/pii/0029554X76901816.

Reference V

[12] Z. Kohley et al. “Modeling interactions of intermediate-energy neutrons in a plastic scintillator array with Geant4”. In: *Nuclear Instruments and Methods in Physics Research Section A: Accelerators, Spectrometers, Detectors and Associated Equipment* 682 (2012), pp. 59–65. ISSN: 0168-9002. DOI: https://doi.org/10.1016/j.nima.2012.04.060. URL: https://www.sciencedirect.com/science/article/pii/S0168900212004329.

[13] R. Bradford et al. “A New parameterization of the nucleon elastic form-factors”. In: *Nucl. Phys. B Proc. Suppl.* 159 (2006). Ed. by F. Cavanna, J. G. Morfin, and T. Nakaya, pp. 127–132. DOI: 10.1016/j.nuclphysbps.2006.08.028. arXiv: hep-ex/0602017.

Reference VI

[14] Aaron S. Meyer et al. "Deuterium target data for precision neutrino-nucleus cross sections". In: *Phys. Rev. D* 93.11 (2016), p. 113015. DOI: 10.1103/PhysRevD.93.113015. arXiv: 1603.03048 [hep-ph].

[15] A. Bodek et al. "Vector and Axial Nucleon Form Factors:A Duality Constrained Parameterization". In: *Eur. Phys. J. C* 53 (2008), pp. 349–354. DOI: 10.1140/epjc/s10052-007-0491-4. arXiv: 0708.1946 [hep-ex].

[16] Huey-Wen Lin. "Nucleon helicity generalized parton distribution at physical pion mass from lattice QCD". In: *Phys. Lett. B* 824 (2022), p. 136821. DOI: 10.1016/j.physletb.2021.136821. arXiv: 2112.07519 [hep-lat].

Backup

Event Rate with Constrained Backgrounds

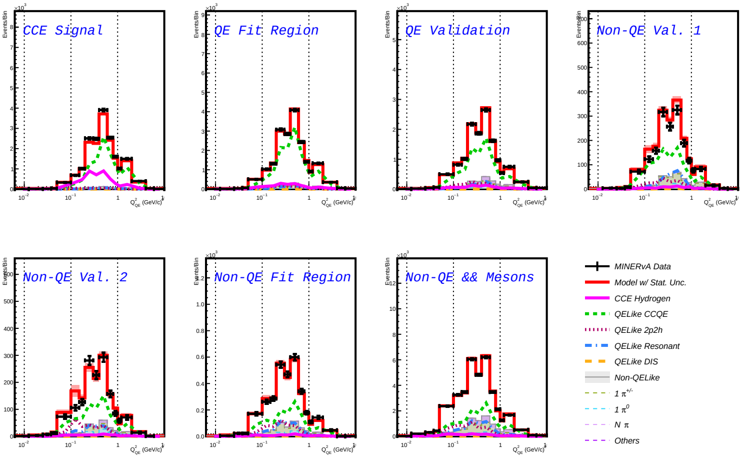

Event Rate with Constrained Backgrounds

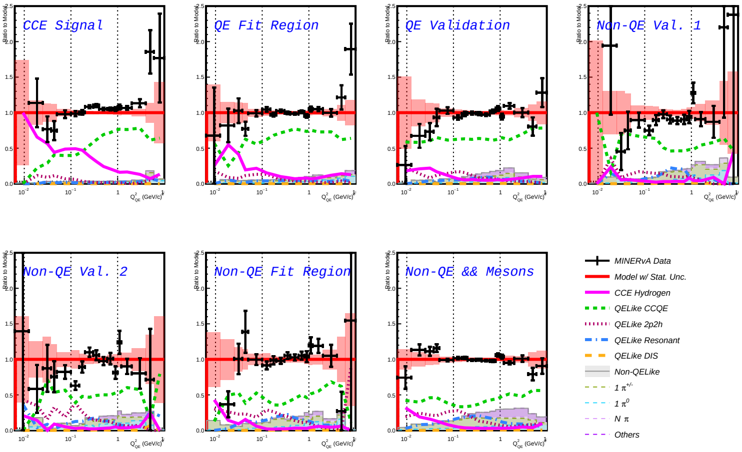

z-expansion parameters

z-expansion formalism and constraints on a_k

$$F_{\mathrm{A}}(Q^2) = \sum_{k=0}^{k_{\mathrm{max}}} a_k z^k$$

$$z = \frac{\sqrt{t_{\mathrm{cut}} + Q^2} - \sqrt{t_{\mathrm{cut}} - t_0}}{\sqrt{t_{\mathrm{cut}} + Q^2} + \sqrt{t_{\mathrm{cut}} - t_0}}$$

$$\sum_{k=n}^{\infty} k(k-1)\ldots(k-n+1)a_k = 0, n \in (0,1,2,3)$$

$$\chi^2 = \Delta X \cdot \mathrm{cov}^{-1} \cdot \Delta X + \lambda \left[\sum_{k=1}^{5} \left(\frac{a_k}{5a_0} \right)^2 + \sum_{k=5}^{k_{\mathrm{max}}} \left(\frac{k a_k}{25 a_0} \right)^2 \right]$$

Central value fit: $k_{\mathrm{max}} = 8, \lambda = 0.13$

Dipole Fit

- $M_A = 1.15(10)$ GeV
- Fit $\chi^2 = 10.2$
- Comparable with z-expansion fit
  - $k_{\max} = 6$
  - $\lambda = 0$
  - $\chi^2 = 9.64$

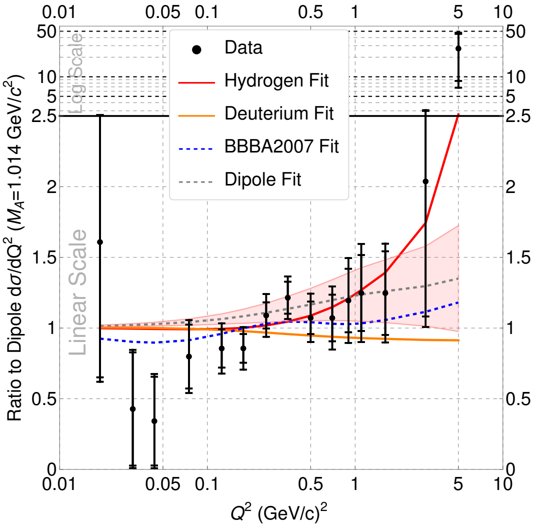

$\delta\theta_{\mathrm{P}}$ and $\delta\theta_{\mathrm{R}}$

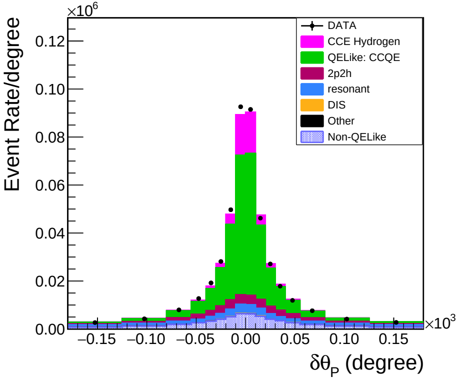

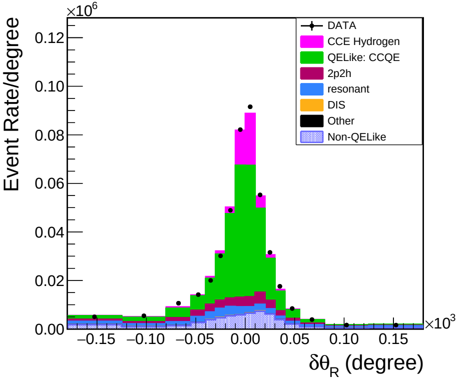

Neutrino Mode Check

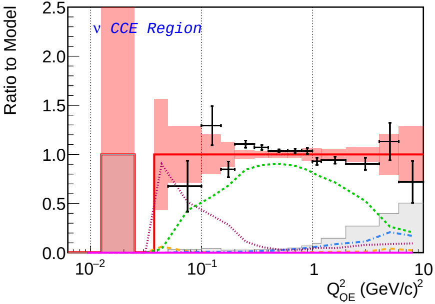

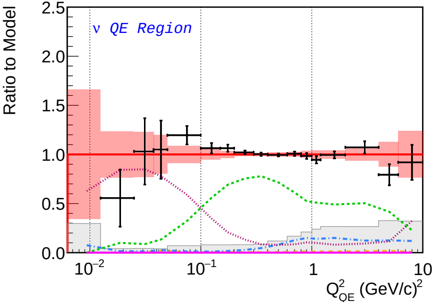

We select events with trackable protons in the neutrino mode, and apply the same fitting mechanism on the non-CCE regions. Data and MC mostly agree within uncertainty. The slight MC deficiency in the ν CCE region can be explained the uncertainty in the 2p2h (next slide).

Neutrino Mode Check II

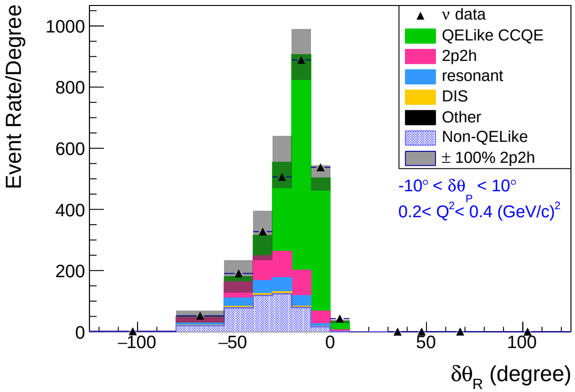

A 100% 2p2h uncertainty covers the data. In the $\bar{\nu}$ mode a 100% 2p2h uncertainty is adequately covered by the total uncertainties.